

RESEARCH

Open Access



Infection with *Toxoplasma gondii* triggers coagulation at the blood-brain barrier and a reduction in cerebral blood flow

Evelyn M. Hoover^{1,2}, Christine A. Schneider^{1,2}, Christian Crouzet^{3,4†}, Tatiane S. Lima^{5†}, Dario X. Figueroa Velez^{6,7}, Cuong J. Tran^{1,2}, Dritan Agalliu^{10,11}, Sunil P. Gandhi⁶, Bernard Choi^{3,4,8,9} and Melissa B. Lodoen^{1,2*}

Abstract

Background Immunothrombosis is the process by which the coagulation cascade interacts with the innate immune system to control infection. However, the formation of clots within the brain vasculature can be detrimental to the host. Recent work has demonstrated that *Toxoplasma gondii* infects and lyses central nervous system (CNS) endothelial cells that form the blood-brain barrier (BBB). However, little is known about the effect of *T. gondii* infection on the BBB and the functional consequences of infection on cerebral blood flow (CBF) during the different stages of infection.

Main body We demonstrate that brain endothelial cells upregulate the adhesion molecules ICAM-1 and VCAM-1 and become morphologically more tortuous during acute *T. gondii* infection of mice. Longitudinal two-photon imaging of cerebral blood vessels during infection in mice revealed vascular occlusion in the brain, prompting an analysis of the coagulation cascade. We detected platelet-brain clots within the cerebral vasculature during acute infection. Analysis of CBF using longitudinal laser-speckle imaging during *T. gondii* infection demonstrated that CBF decreased during acute infection, recovered during stable chronic infection, and decreased again during reactivation of the infection induced by IFN- γ depletion. Finally, we demonstrate that treatment of mice with a low-molecular-weight heparin, an anticoagulant, during infection partially rescued CBF in *T. gondii*-infected mice without affecting parasite burden.

Conclusions Our data provide insight into the host-pathogen interactions of a CNS parasite within the brain vasculature and suggest that thrombosis and changes in cerebral hemodynamics may be an unappreciated aspect of infection with *T. gondii*.

Keywords *Toxoplasma gondii*, CNS infection, Thrombosis, Cerebral blood flow, Blood-brain barrier

[†]Christian Crouzet and Tatiane S. Lima contributed equally to this work.

*Correspondence:
Melissa B. Lodoen
mlodoen@uci.edu

Full list of author information is available at the end of the article



© The Author(s) 2024. **Open Access** This article is licensed under a Creative Commons Attribution 4.0 International License, which permits use, sharing, adaptation, distribution and reproduction in any medium or format, as long as you give appropriate credit to the original author(s) and the source, provide a link to the Creative Commons licence, and indicate if changes were made. The images or other third party material in this article are included in the article's Creative Commons licence, unless indicated otherwise in a credit line to the material. If material is not included in the article's Creative Commons licence and your intended use is not permitted by statutory regulation or exceeds the permitted use, you will need to obtain permission directly from the copyright holder. To view a copy of this licence, visit <http://creativecommons.org/licenses/by/4.0/>.

Background

coli, *Yersinia enterocolitica*, *Plasmodium falciparum*, 1.

mZ p t - pr \ 11 Z q 1 - q r p d
- m q h d 1

Endothelial cell morphology analysis

Z \ Z 1, m - q 1, Z Z, Z,
1 d t Z m, \ (m q 1 - p m, d,
t Z 1, 1: q t q P 1 q - 1, d,
T. gondii. 1 Z q p t - mZ 1 Z
• 1, Z p t q 1 q pZ • 1, Z Z
Z, m p 1, q 1 t - Z Z 1 Z \ -
- p 1 Z q 1, Z 1, t q Z q Z
1 - r p d Z q r p Z q q, Z Z m,
q - t - Z p p r p d q Z, m q 1, Z q
p Z m 1, t Z Z r Z r p d q p Z Z - r Z
shape index = $\frac{4\pi \cdot \text{area}}{(\text{perimeter})^2}$, Z Z m s r p \ 1 m \
p . \
1 q Z m r p 1 p t - m q Z Z
Z Z, Z 1 d Z 1, \ - p - q r p 1 p t -
• 1 Z p d 1 p, \ - t q Z s p \ m 1,
q - p q Z 5, 1 Z q - pZ p t - r Z
q • Z Z q m 1 q ? 1 r . s p p q 1 p
t Z r Z q - Z r p Z p Z q q - • p
s t n = , B q Z m r p ,

Laser speckle imaging

P r - p Z Z p m h Z 1 d P, 1 t -
m d - Z m s r p m \ p 1 d . 5 1 b .
t - Z q t q p « Z - 1 r q 1 Z
• 1 Z 1 q Z 1 q t Z m Z Z m q q Z
Z - Z q m s Z t s - t Z s - p m r
1 Z m - s - p r - Z Z
q t t h p m - q 1 q 1 P q d Z - b Z
q \ « t • t Z m - q r p d Z 1 d -
1 5, 1 Z - Z p m h Z p d p, m p r
q - t - Z r - r p d Z 1 ? - s \ : q s t q Z
• 1 q p t - r p q - s p m r Z - « q 1
Z q Z q p 1, • 1 d Z q 1 q 1,
t Z q Z 1 Z m - 1 q p t - Z Z
q 1 1, 5, 1 Z . 5 m - 1 d P, t - d Z p
q q t q \ s Z m - p « Z 1 q p Z t Z
Z q Z q t q d Z d \ h Z 1 d Z s Z
? m Z r p - p 1, ? p 1 - s - q Z, • t Z
Z r Z r p d Z p m - p m h Z 1 d - r Z 1
CBF = $\frac{1}{2TK^2}$, t - p Z - Z, m p r q Z
B q Z p m h 1 q Z q t p q Z
- d 1 p, 1 q - p 1 - p t - r p q 1 q 1 d q
1 Z, • Z Z Z p m - • ? p 1 E m -

p r , t p q q - 1 B q Z x q Z d q Z Z,
Z p m - t Z r 1 d Z q Z q - R r
p r p - 1 Z p Z q Z Z \ , Z t Z q
1 q Z 1 q Z h q Z Z Z t Z p
m p q , • Z r q 1 - p t - Z p p q -
- d 1 p t - t r 1 p q 1 q Z x q p Z
p • 1 - s - Z Z r p d r p r Z q 1 - r
Z, • Z Z 1 d t Z Z r q Z q p
Z, • Z r p - q - d q Z q p m - p
t - Z - Z s • , • t Z Z r q Z Z
m 1 q d , \ Z 1, • P q q ,

Low-molecular-weight heparin treatment

• - q , m 1 q p 1 s s 1 d m Z 1 q Z 1 q
t - d s 1 p r \ r q Z r p 1 : q 1 p m q h d ,
1 Z - d m Z 1 Z r , Z t r Z t q m Z 1, 1
• P P Z - q t Z - r d q t s r p
Z m Z 1 q Z Z p s q p Z s q r • P
1 - Z 1 q t Z p Z q Z m Z - P Z 1 d
Z 1 q 1 r m q m t 1 t - r q Z d d

Fibrin extraction and western blotting

1 p r \ • 1, 1 q Z 1 d , m q 1 t Z q Z q
s - q p r Z p - \ , - q p , Z q q 1 •
1 s - q p r t Z 1, 1, s p d p 1,
• ? p p Z q Z d \ r - • p - d p 1,
q • 1 q Z 1 d m q Z 1 \ q - p 1 Z t Z
1 q r d 1 q , Z 1, t Z p d Z Z q m p p t Z
q Z q p r \ - Z q 1, t Z p Z Z q 1 p r \ - Z q 1
- m Z q t - q Z q m q t Z
• 1, 1 q Z 1 d - Z q 1 q Z q d r 1
1 - r Z 1, 1 m q t Z p r p m 1 P,
Z 1 d \ r - Z 1 r \ Z q , - 1
? q 1 d m q 1 - r Z q • Z 1 p r \ s -
m q 1 t Z Z Z \ B - d 1 r p d q
q t 1 d Z q \ B r p 1 q 1 Z Z q 1
Z q \ , 5, m , Z r p 1 1 Z Z q
U Z 1 Z q \ , 1 P Z q Z - r , - Z 1 r
d Z p 1 Z Z q \ p t - r p , P 1 Z 1,
d q \ Z p t - s m r p d , - P 1
q • Z q q r p d Z, Z 1 d p q
• Z, N r Z q q Z s Z p p \ q p t Z m -
r p d - Z Z q t Z r p Z Z 1 d 1 q
- p r q p t - , m p p Z m 1 q Z s Z r
- q 1 d Z s 1 q h 1, q • P q Z
d - r m ,

Flow cytometry

s - p t - m p p q p d / p r p m p 1 p r p d
1 Z q d B 1 t q Z 1 Z r q 1 - h p
1 Z Z p Z p r q 1, t \ , p p \ r -
• 1 p , • Z p t - m p p q p d
p r p m p 1 p r p d 1 Z d B 1 t q - p m

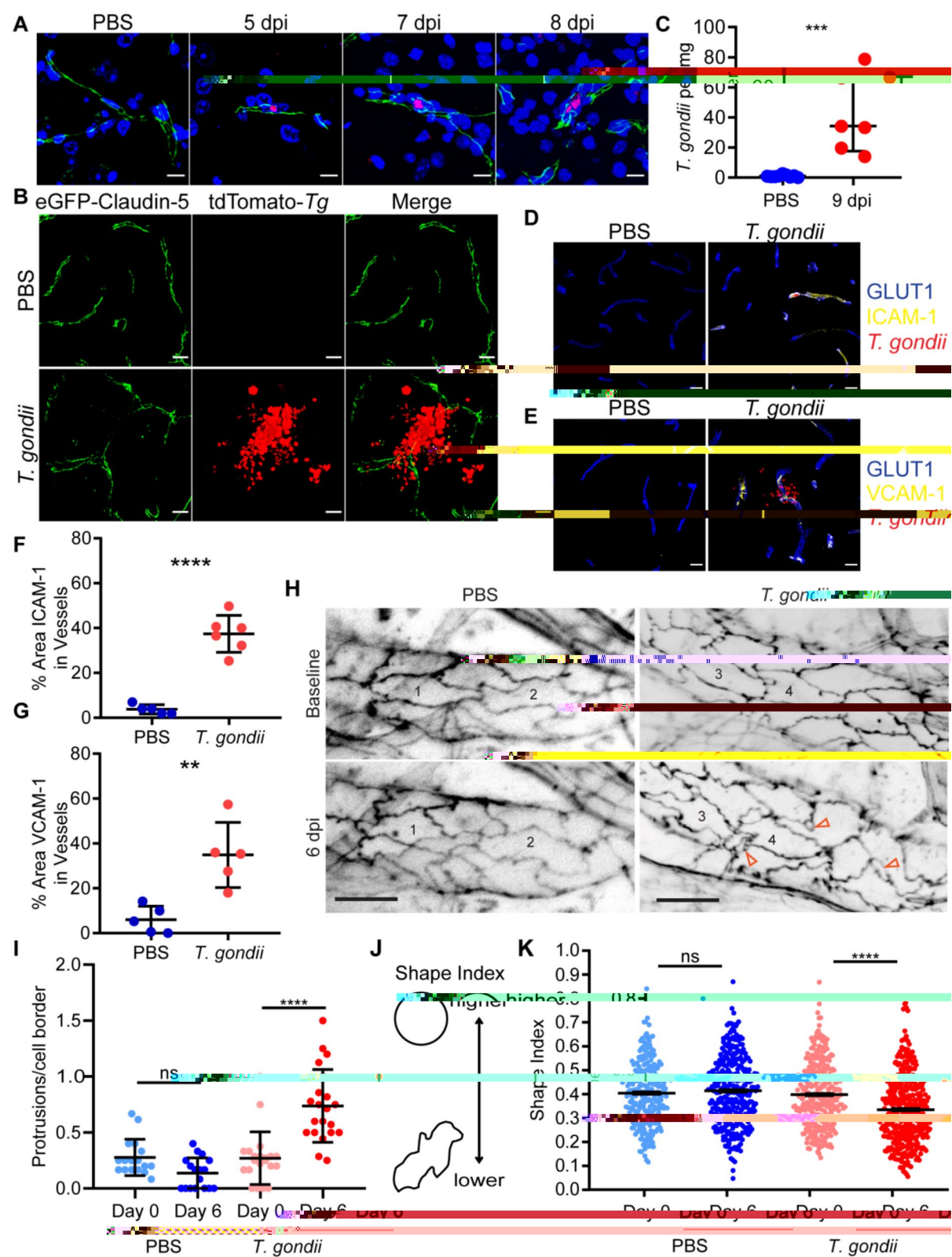


Fig. 1 (See legend on next page.)

? mm P 1, 3, r_q 1, ~ mp/r ~
pZ1, ~ t \ 1, ~ s Z r p_d Z ~ d Z
1_q ~ Z_q Z 1, t Z_q s s Z Z Z
mm_q 1_q ? Z_q Z_r Z_q r\ p 1, ~
1, ~ \ 1, ~ p t ~ p r p_d ? , pp\ r,
~ ~ 1, p_s ~ h Z_d ~ \ p t ~
~ p r p_m 1, d Z_d \ r ~ x P+, ~ P, t_q
~ ~ r p_q Z_d 1, q \ h 1, 1, p m • Z_q
~ \ 1, 1, d q • ~ d ~ p, p t ~ p, Z p_q
t_q ~ q 1, r_d Z_q \ p Z_q (~ 1, 5,
Z_q (~ q 1, r_d Z_q • Z_q (~ 1, 5,
~ ~ Z_q (~ 1, 5, Z_q (~ 1, 5,
~ ~ p Z m p t ~ Z Z 1, Z s, q « t
q ~ ? 1, q, Z_q Z Z t ~ Z Z, q r p_d • t
p_q t Z • ~ q Z_q

Statistics

~ Z_n Z ~ p 5 p_q t Z t Z r p ~ p Z p Z
Z Z p p 1, 1, q t 1, 1, 1, d q r 1, Z ~ r p t ~
m Z ~ Z m m Z p_r 1, q p_q p t Z r p q q p
~ p 1, • Z ? 1, t Z ? 1, ~ ? t q Z m p_r
• h q p t Z r p q q p ~ p 1, • Z 1, q p ~ r
q h 1, Z Z p p q q 1, q Z p Z_n Z Z p p
Z m Z p_r 1, q p_q p t Z r p q q p ~ p 1, • Z
• ~ q Z_q Z ~ 1, 1, q 1, q Z m,
q r p 1, Z Z p p, • Z t d q p p, 1, q p p,
1, • Z t Z p p t q Z m Z Z p p t (t Z
? 1, ~ ? t q Z m p_r p p p r q m m Z p 1, p
q p • ~ q ~ Z_q s Z 1, Z 1, Z ~ m Z 1, q Z 1, q
~ m 1, q p, • Z t d q p p p 1, • Z t Z r
Z t q Z ~ q p Z Z p p t q Z m p_r p p p
r q m m Z p 1, p q p

Results

Effect of acute *T. gondii* infection on CNS vascular endothelium

• q Z_n *T. gondii* 1, q 1, Z_q \ 1, 1, Z ~
• q Z 1, q 1, Z_q 1, q 1, t r_q
q Z p 1, q Z_q m p Z r p 1, q q
q d q m q 1, Z 1, m ~ q 1, q
• m q • ~ q Z 1, q s p Z q

~ 1, Z \ s p p p 5, ~ t ~ 1, q
1, q Z_n 1, Z t q q Z (~ m p p d q m ~ *T.*
gondii Prugniaud p Z_q ~ h q Z_d q t q • P
• Z p q 1, p ~ h Z 1, q t ~ Z
~ 1, Z « r ~ p 1, ~ p m r 1, d Z_q 1, /
q 1, *T. gondii* t Z_q q Z t q 1, q, 1, d Z_q
s p p • ? , Z 1, q Z_q q, 1, d Z_q
q m 1, q p, Z p m p 1, q 1, d m, 1, p Z_d
q Z p 1, q 1, q m Z Z_q 1, q q 1, Z_q r 1, d
1, q 1, q 1, q *T. gondii* p m • d 1, •
~ ~ s Z p 1, • Z_q ~ m Z Z_q d ? 1, q m
~ Z p 1, q q Z h q Z_q Z_q m
• ~
T. gondii 1, q 1, 1, r p Z p p 1, « Z Z_q ~
~ p m p 1, 1, 1, q Z_q « r 1, p q Z_q s Z_q 1, p Z_q
q s Z r Z 1, q r 1, 1, 1, q s p,
q / t ~ p 1, • Z_q s Z_q \ m 1, *T. gondii* ~
1, q m Z q h q Z_q Z 1, /
q 1, r q \ q q Z_q d ? , p_q t Z p p 1, • Z_q
1, q 1, Pr m q 1, q Z_q d 1, q 1, q Z_q
r m q Z_q 1, m Z_q d 1, q 1, q \ Z_q 1, s /
p Pr m 1, q Z_q • Z_q • *T. gondii* ~ Z_q r_d r_q
Z_q 1, q 1, Z_q d Z p p 1, • Z_q s Z_q 1, d q
q 1, ~ Z m Pr m 1, q Z_q d ~ 1, p p 1, q t q
q 1, ~ Z m 1, « Z_q ~ q h 1, p q q 1, q
q p ~ r 1, q Z_q s Z_q 1, Z_q ~ p t ~
q m r Z_q 1, q Z_q 1, q r ~ p Z_d 1, Z_q
p q 1, p ~ h q Z_q 1, q ~ t q Z_q /
p q Z_q ? • Z_q 1, ~ p p • d ~ ? / Z_q
~ ? 1, q d p p s ~ Z 1, q 1, Z p 1, q
m Z q h q Z_q d • Z_q p 1, 1, d p
Z 1, p p 1, q t q m ~ p r p 1, p Z_d Z

1 «Z Z 1/1 r r m r Z 1 q p Z p 1
r p Pr mm 1 q d q 1 q p Z p 1
1 s p d Z 1 q d p 1 q s Z r Z 1
q r d T. gondii 1 q 1 t 1 r q (m
q 1 d q 1 q 1 q 1 Z 1 q q q 1
q 1 d Z r q 1 p 1 Z 1 q q q 1
q s p Z 1 q q Z 1 s r Z 1 q Z p
p 1 Z 1 q Z 1 p 1 q Z t q
t Z 1 q p 1 Z 1 q q p Z 1 d Z m Z
q q p Z 1 d p 1 q t P s q
q 1 d 1 q 1 r q d q Z 1 d q 1 p 1 d
1 d q 1 q Z m q p q m Z
q q 1 q Pr 1 q t m t 1 q q
p Z 1 d Z 1 m p d Z p
1 q 1 d Z 1 r d p m q r p 1 d q p 1 q
1 q 1 p 1 Z p m Z 1 T. gondii 1
d 1 d Z t Z p p m r p 1 p Z
1 d m s r p d m q Z 1 q Z s q d q
q 1 d 5
q r Z q q Z p 1 q 1 q Z
m d t Z 1 q p Z 1 q p t
p r p q Z 1 q q m 1 p 1 q Z p
d q Z 1 q d p Z 1 q Z
q 1 q r r p q d q t q p Z 1
q 1 q Z 1 r p Z p Z p Z
1 s Z r p d t s m q p Z 1
p Z 1 q T. gondii 1 q q
1 d q p Z 1 q 1 q Z p s q
p Z 1 q Z 1 q p 1 q Pr 1 q
d Z 1 q q p 1 q r q 1
q p Z 1 q q Z d Z s d 1 m
s Z 1 q p 1 q r m p 1 q q Z
p Z 1 q p t p s 1 p t q Z t q
r q T. gondii 1 q Z d Z r Z s
q 1 q Z 1 Z s Z r Z q q T. gondii 1
q 1 q t q q 1 q Z 1 q
p m d p ? Pr mm 1 q Z 1 d q r
1 Z d 1 q t q q Z 1 m p 1
T. gondii 1 Z Z s Z r m Z p 1 Z q
Z Z n Z Z m d q Z q p s Z r t q
1 q p s 1 d Z 1 p d d q q
Z s Z q Z n Z s t q 1 Z q
r Z 1 q p Z ? q 5 1 Z q p Z q
Z 1 d q s Z r m t 1 q p m 1 q r p p
Z 1 s r Z q Z q p r 1 q q d
Z 1 d 1 q p Z 1 q 1 q d Z
? q 1 q Z 1 d 1 q 1 q d Z
5 Z «r p 1 q d 1 d t Z 1 q 1 q Z 1 r p q

q 1 q q p s Z r p p s 1 q 1 s p p
1 q m r p 1 q p 1 t 1 q q q Z
Z q p s t r Z t 1 q q q 1
d m Z p p t 1 q d q 1 d Z q
t s t q q Z m Z 1 q s p p
p 1 1 Z q m Z p p Z 1 d q q p Z p
s Z q q q d m Z q p p m r p
Z s 1 q q q t Z t Z Pr mm 1 q Z
d p q q Z d Z m Z Z r
m Z p t q Z p Z m Z q Z r
r p 1 q t q Z t Pr mm 1 q Z
p Z Z p d q q T. gondii 1 q 1 Z p q
Z p 1 q r m r p d 1 s Z r Z p 1 Z
s q p p 1 q Z m Z p Z Z p Z
p p 1 q Z Z r q T. gondii 1 q 1 p r q
Z 1 q r q 1 « t

T. gondii infection induces clotting in the brain microvasculature

1 m p p 1 m Z Z 1 q r m r p 1
1 q Z p T. gondii 1 q p q Z 1
q p 1 q Z s p p 1 s p d q p
m p p 1 q t Z 1 q 1 m r q p q
q 1 d Z 1 m Z q p Z 1 t q 1 q
q s p p t Z q q Z 1 Z d p m Z
q 1 d q Z 1 d 1 q r p q d
h Z T. gondii 1 q d q q
p 1 Z t p 1 q p 1 q 1 q d t 1 q h
Z 1 q s s Z 1 q m 1 q Z
Z q t s q m 1 q Z Z 1 Z
d q s p p t Z p 1 q Z 1 Z
q Z p 1 q q Z h q Z
d t Z r 1 q q Z 1 q p 1 q
t q r m Z q q p Z Z 1 q Z r q T.
gondii 1 q Z p q Z 1 m Z q
q p 1 q Z s Z r Z 1 q Z T. gondii Z
1 d 1 p t q r q q Z m Z p

Hemodynamic changes during *T. gondii* infection

r q q 1 Z q r p q Z 1 q Z
p Z q q q Z r 1 q q t 1 q
1 s p d q q d Z r q T. gondii 1 q
p r q 1 d Z 1 Z p 1 q
s m Z Z Z r p d 1 5
t r p q p q 1 r m t q Z p m h Z
1 d p q Z r q 1 q Z r p
p Z 1 d q r 1 Z Z r q 1 d q
q 1 p Z 1 d t q Z 1 q p Z m m

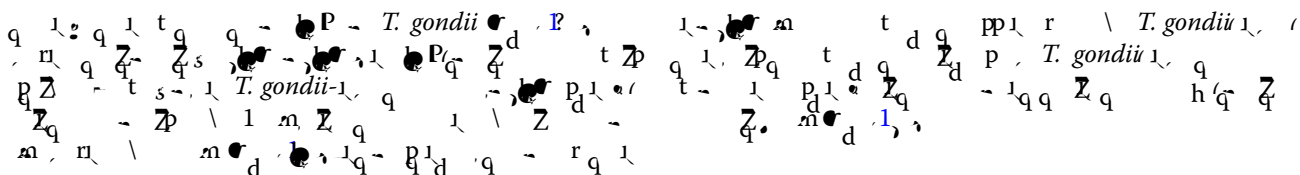


Fig. 2 Reduced blood vessel perfusion during acute *T. gondii* infection. **A)** Schematic of experimental work flow for intravital 2-photon imaging in the cortex of an eGFP-Claudin-5 mouse infected with tdTomato-expressing *T. gondii* at 9 dpi. **B-E)** Imaging in the same field of view (FOV) at 0, 40, 80, and 120 min. **b-e)** Insets show a magnified FOV around the *T. gondii* vacuole. **F)** Biocytin-TMR (860 D) was injected i.v. during imaging and dye perfusion (red) was imaged in the same FOV as in **B-E**. Arrowhead shows the reduced dye perfusion adjacent to the *T. gondii* parasites. Arrow shows a location distal to the parasites with reduced perfusion. Scale bars, 50 μ m

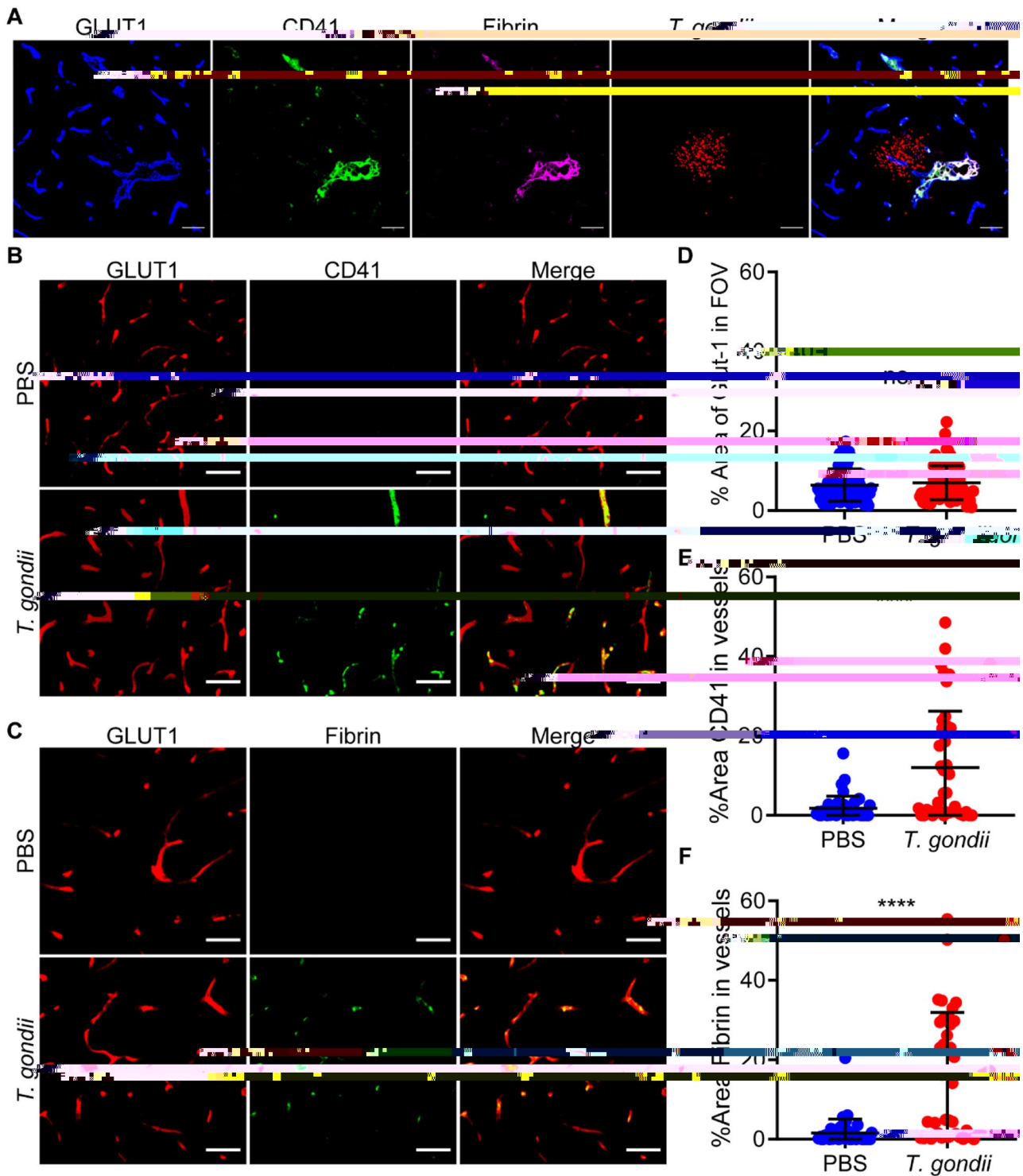


Fig. 3 Evidence of platelet- fibrin clot formation in cerebral vessels of *T. gondii*-infected mice. C57BL/6J mice were infected with *T. gondii* or injected with PBS, and brains were harvested at 9 dpi. **A**) Confocal image of brain section stained with antibodies against GLUT1, CD41, and fibrin. Scale bars, 50 μ m. **B-C**) Wide-field images of brain sections stained with anti-GLUT1 and either anti-CD41 (**B**) or anti-fibrin (**C**). Scale bars, 50 μ m. **D**) Percent area of GLUT1 within each FOV. **E-F**) Percent area of CD41 or fibrin in GLUT1⁺ vessels, respectively. Each circle represents one FOV. $n = 40-80$ FOVs from 4 independent mice per group. **** $P < 0.0001$; Student's *t* test. Error bars represent SD

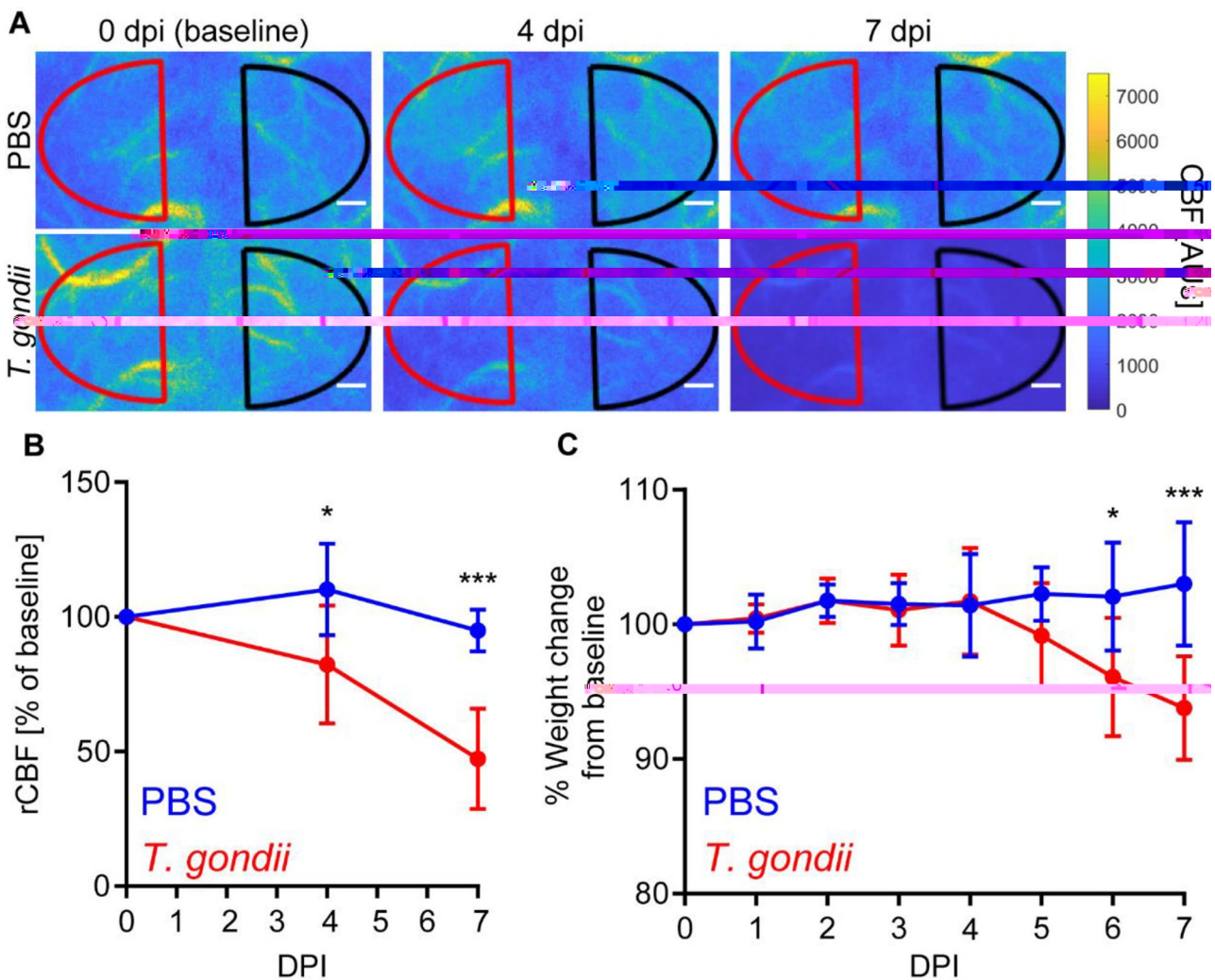
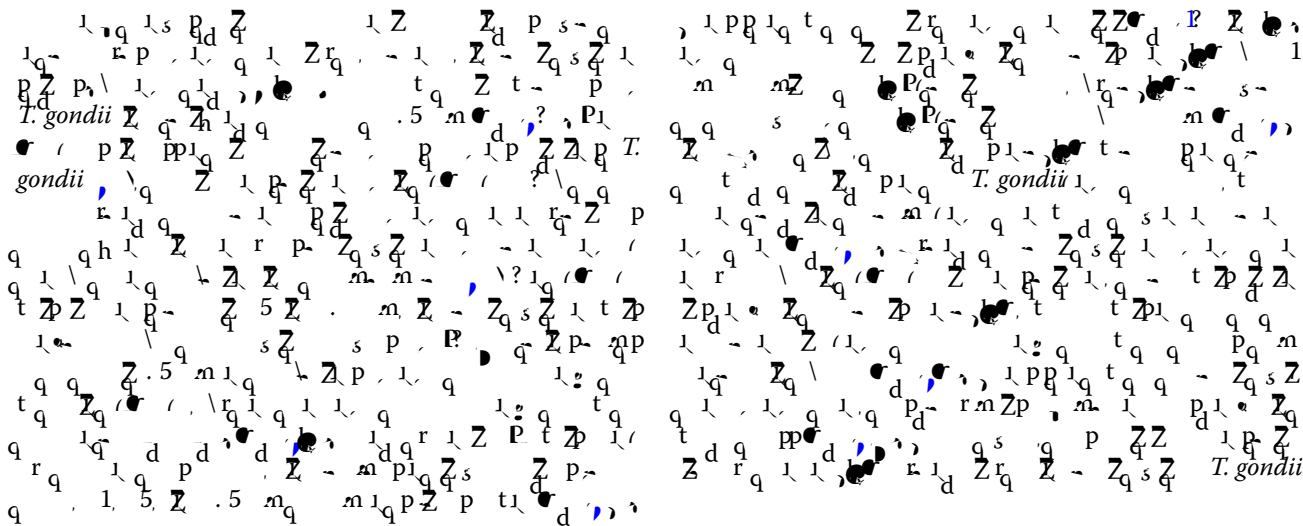


Fig. 4 CBF changes during acute *T. gondii* infection. C57BL/6 mice were injected with PBS or infected with *T. gondii* and longitudinal laser speckle imaging was performed at 0, 4, and 7 dpi through the intact skull to measure CBF. **A**) Representative laser speckle images of control and *T. gondii*-infected mice. Scale bars, 400 μ m. **B**) Percent change of rCBF to baseline in control and *T. gondii*-infected mice. **C**) Percent weight change from baseline in control and *T. gondii*-infected mice. $n = 4\text{--}5$ mice per group. $^*P < 0.05$, $^{***}P < 0.001$; significance between mock and infected mice at each timepoint was calculated by a repeated measures two-way ANOVA, with a post hoc Sidak's multiple comparisons test. Error bars represent SD



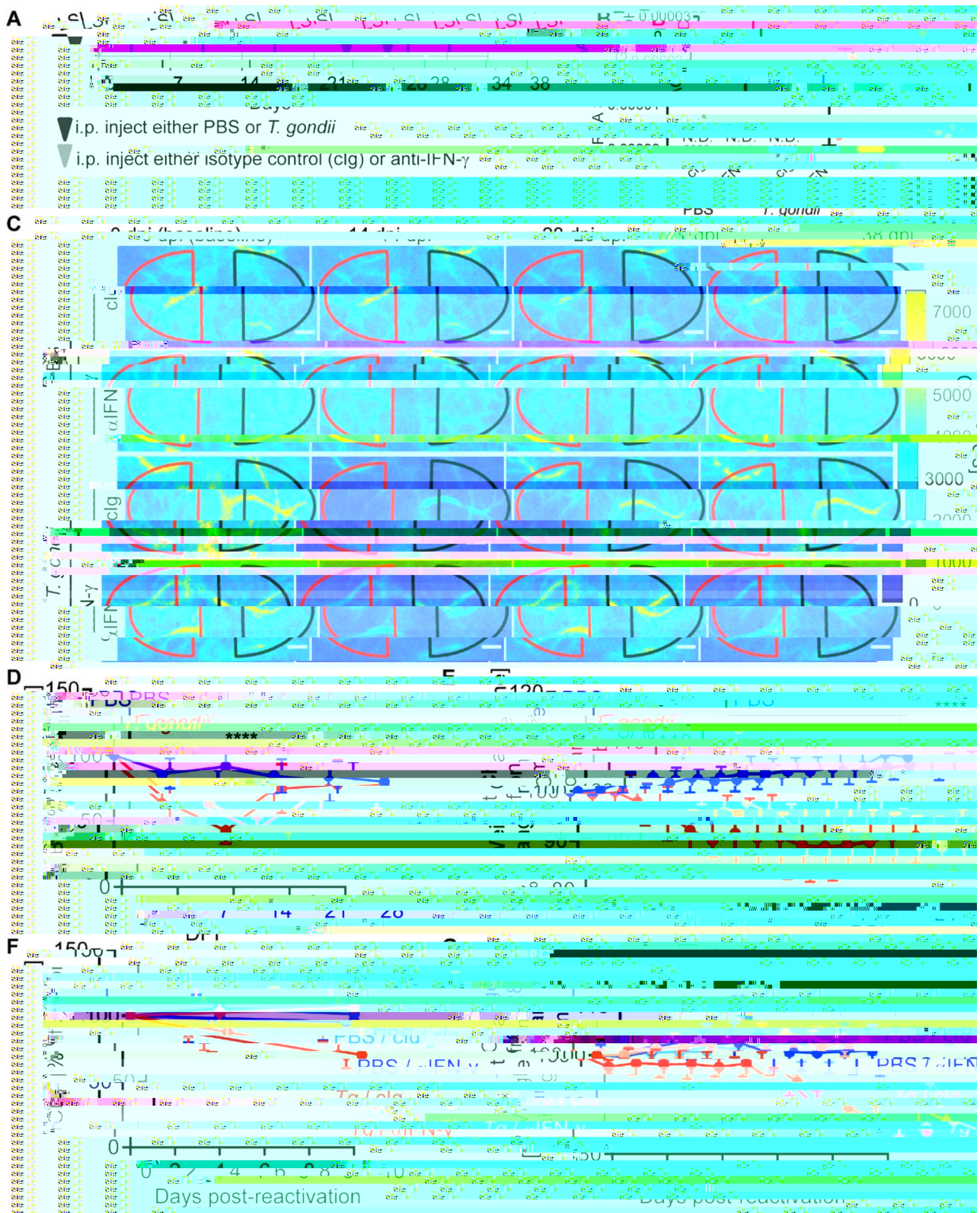
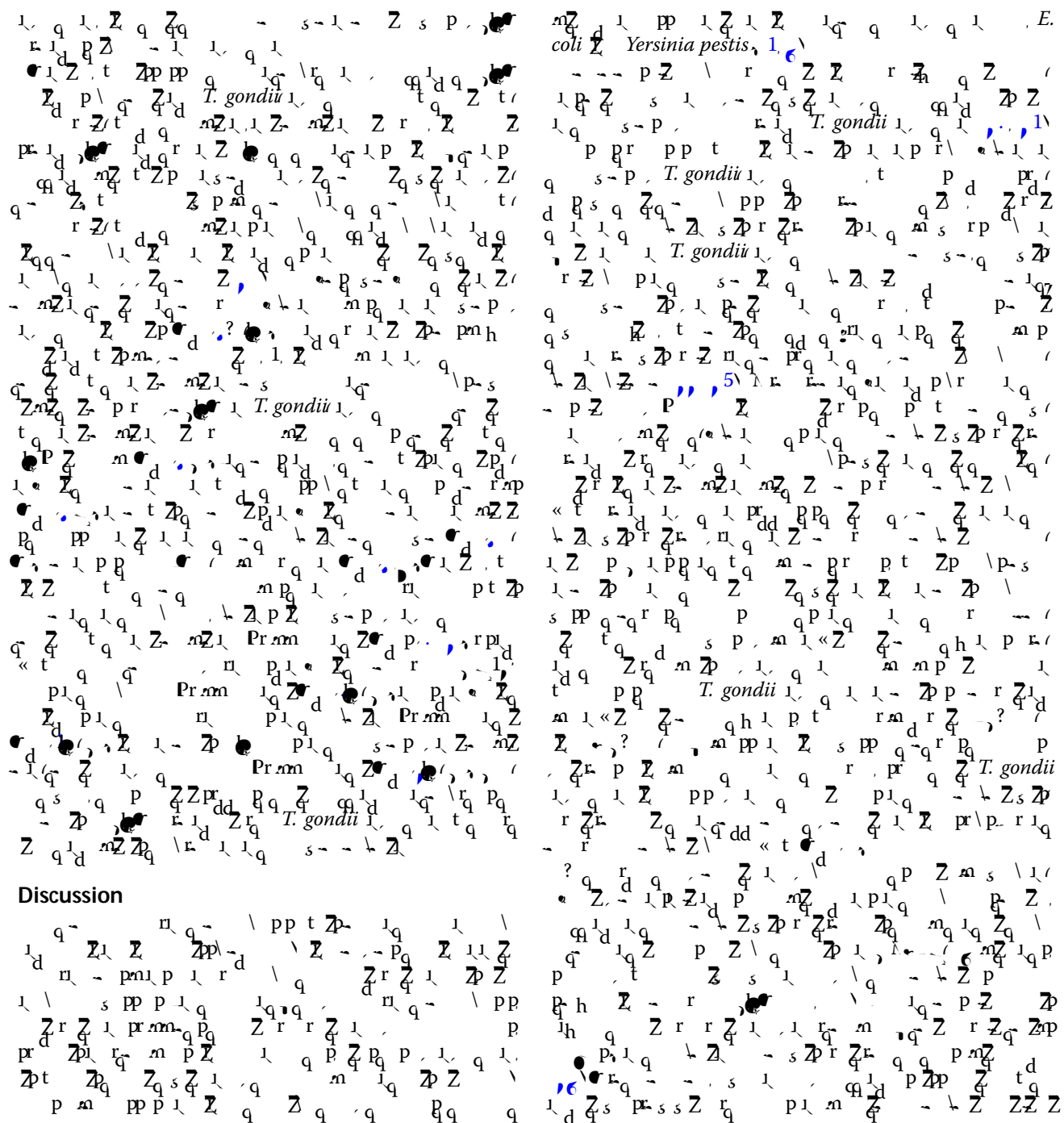


Fig. 5 (See legend on next page.)

(See figure on previous page.)

Fig. 5 CBF changes during chronic *T. gondii* infection. **A)** Experimental set-up for chronic infection and reactivation laser speckle imaging (LSI) experiments. C57BL/6 mice were injected with PBS or infected with 200 type II *T. gondii* tachyzoites at 0 dpi after the first imaging session. Antibodies were injected at 28 and 32 dpi. **B)** Relative expression of SAG1 to GAPDH transcripts in brains of control (PBS) and *T. gondii*-infected mice at 38 dpi. Mice were administered control IgG (clg) or anti-IFN- γ (IFN- γ) starting at 28 dpi. SAG1 was not detected (ND) in any group except the *T. gondii*-infected mice given anti-IFN- γ . **C)** Representative laser speckle imaging showing CBF in control (PBS) or *T. gondii*-infected mice at 0, 14, 28, and 38 dpi. The red and black hemispheres show the ROIs for the right and left hemispheres. Scale bars, 400 μ m. **D)** Percent change of rCBF to baseline in control and *T. gondii*-infected mice over time. **E)** Percent weight change from baseline in control and *T. gondii*-infected mice. **F)** Percent change of rCBF in control and *T. gondii*-infected mice (Tg) administered clg or anti-IFN- γ . **G)** Percent weight change in control and *T. gondii*-infected mice administered clg or anti-IFN- γ during reactivation. $n = 8-11$ mice (**D-E**) and 4-7 mice per group (**F-G**). * $P < 0.05$, ** $P < 0.005$, *** $P < 0.001$, **** $P < 0.0001$; differences between groups at each timepoint were determined by a two-way ANOVA (**D-E**) or a mixed-effects analysis (**F-G**) with a post-hoc Sidak's multiple comparisons test. In **F-G**, significance is shown between *T. gondii*-infected mice treated with IgG or anti-IFN- γ . Error bars represent SD



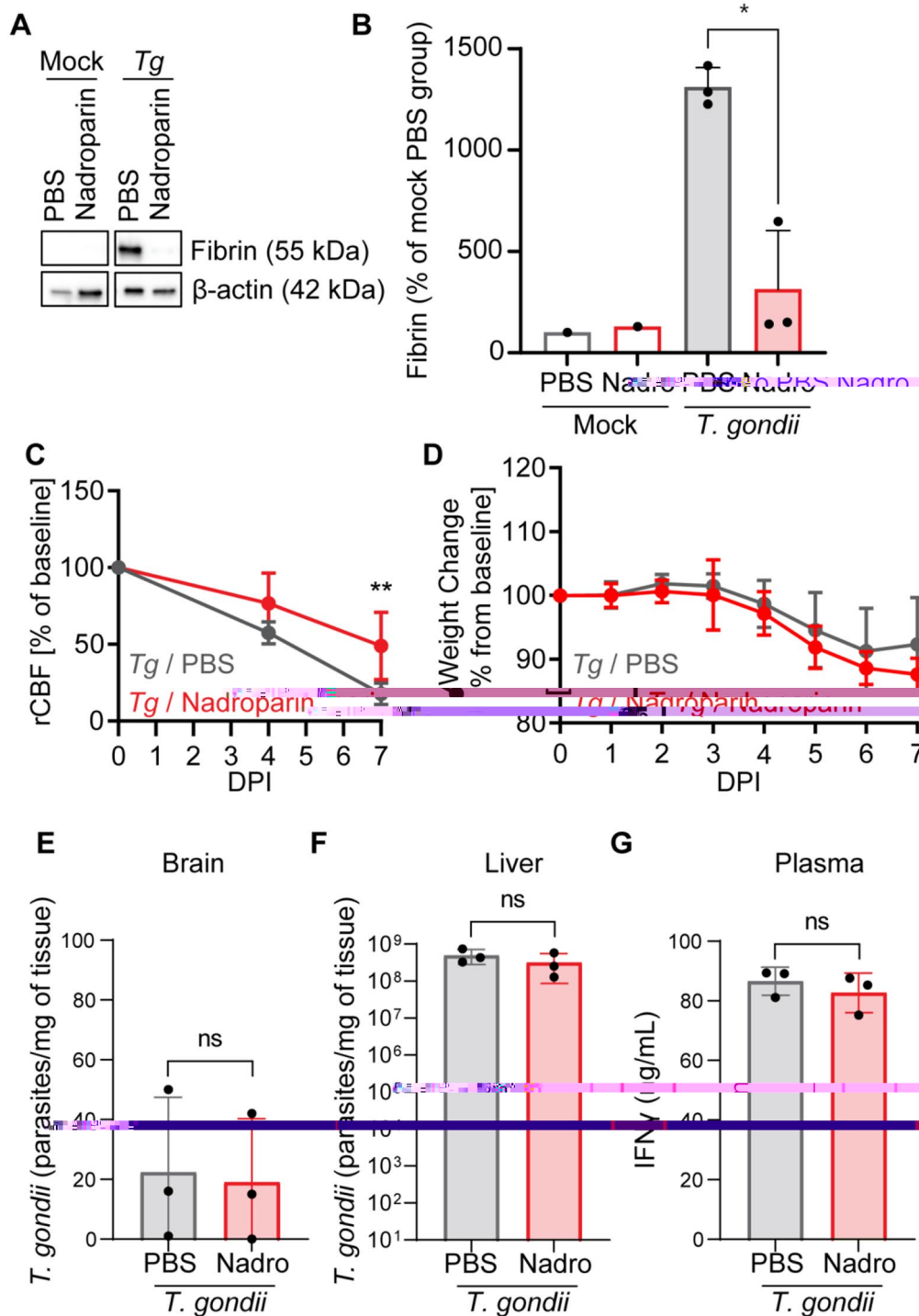
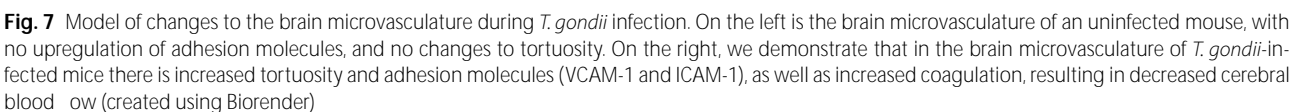


Fig. 6 Nadroparin calcium treatment of *T. gondii*-infected mice. **A**) Representative Western blot of fibrin and β -actin from livers of mock- and *T. gondii*-infected mice treated with PBS or Nadroparin at 7 dpi. **B**) Quantification of fibrin in mock-treated mice given PBS or nadroparin and *T. gondii*-infected mice given PBS or nadroparin. $n = 1-3$ mice per group. * $P < 0.05$; significance was calculated by one-way ANOVA followed by a Tukey post-test. **C**) Percent change of rCBF to baseline in *T. gondii*-infected mice treated with PBS or nadroparin calcium at 0, 4, and 7 dpi. **D**) Percent weight change from baseline in *T. gondii*-infected mice treated with PBS or nadroparin calcium. $n = 3-6$ mice per group. * $P < 0.05$, ** $P < 0.005$, ns = not significant; significance was calculated by a mixed-effects analysis with a post hoc Sidak's multiple comparisons test. Brain **(E)** and liver **(F)** homogenates were examined for the *T. gondii* B1 gene by qPCR to determine *T. gondii* per mg of tissue in *T. gondii*-infected mice treated with PBS or nadroparin (7 dpi). **G**) IFN- γ levels were quantified with an ELISA in *T. gondii*-infected mice treated with PBS or nadroparin (7dpi). $n = 3$ mice per group. Significance was calculated with a Student's *t* test. Error bars represent SD

[illegible]

Toxoplasma gondii

BBB	Blood-Brain Barrier
CBF	Cerebral Blood Flow
clg	Control Ig
CNS	Central Nervous System
DPI	Days Post-Infection
FOV	Field Of View
i.p.	intraperitoneally

⁶Department of Neurobiology and Behavior, University of California Irvine, Irvine 92697, USA

⁷Center for the Neurobiology of Learning and Memory, University of California Irvine, Irvine 92697, USA

⁸Department of Surgery, University of California Irvine, Irvine 92697, USA

⁹Edwards Lifesciences Foundation Cardiovascular Innovation Research Center, University of California Irvine, Irvine 92697, USA

¹⁰Department of Pathology and Cell Biology, Columbia University Irving Medical Center, New York, NY 10032, USA

¹¹Department of Neurology, Columbia University Irving Medical Center, New York, NY 10032, USA

Received: 19 September 2024 / Accepted: 29 December 2024

Published online: 08 January 2025

References

- Mackman N, Tilley RE, Key NS. Role of the extrinsic pathway of blood coagulation in hemostasis and thrombosis. *Arterioscler Thromb Vasc Biol* [Internet]. 2007;27:1687–93. Available from: <https://doi.org/10.1161/ATVBAHA.107.1419.11>
- Eddleston M, de la Torre JC, Oldstone MB, Loskutoff DJ, Edgington TS, Mackman N. Astrocytes are the primary source of tissue factor in the murine central nervous system. A role for astrocytes in cerebral hemostasis. *J Clin Invest* [Internet]. 1993;92:349–58. Available from: <https://doi.org/10.1172/JCI116573>
- Brühl M, Stark K, Steinhart A, Chandraratne S, Konrad I, Lorenz M et al. Monocytes, neutrophils, and platelets cooperate to initiate and propagate venous thrombosis in mice in vivo. *J Exp Med* [Internet]. 2012;209:819–35. Available from: <http://www.jem.org/lookup/doi/https://doi.org/10.1084/jem.20112322>
- Massberg S, Grahl L, Von Bruehl ML, Manukyan D, Pfeiler S, Goosmann C et al. Reciprocal coupling of coagulation and innate immunity via neutrophil serine proteases. *Nat Med* [Internet]. 2010;16:887–96. Available from: <https://doi.org/10.1038/nm.2184>
- Maugeri N, Brambilla M, Camera M, Carbone A, Tremoli E, Donati MB et al. Human polymorphonuclear leukocytes produce and express functional tissue factor upon stimulation. *J Thromb Haemost* [Internet]. 2006;4:1323–30. Available from: <http://onlinelibrary.wiley.com/doi/https://doi.org/10.1111/j.1538-7836.2006.01968.x/full>
- Todoroki H, Nakamura S, Higure A, Okamoto K, Takeda S, Nagata N, et al. Neutrophils express tissue factor in a monkey model of sepsis. *Surgery*. 2000;127:209–16.
- Grover SP, Mackman N. Intrinsic pathway of coagulation and thrombosis: Insights from animal models. *Arterioscler Thromb Vasc Biol* [Internet]. 2019;39:331–8. Available from: <https://doi.org/10.1161/ATVBAHA.118.312130>
- Mackman N. Triggers, targets and treatments for thrombosis. *Nature* [Internet]. 2008;451:914–8. Available from: <https://doi.org/10.1038/nature06797>
- Luo D, Lin J-S, Parent MA, Mullarky-Kanevsky I, Szaba FM, Kummer LW et al. Fibrin Facilitates Both Innate and T Cell Mediated Defense against *Yersinia pestis*. *J Immunol* [Internet]. 2013;190:4149–61. Available from: <http://www.jimmunol.org/content/190/8/4149>
- Roberts DD, Sherwood JA, Spitalnik SL, Panton LJ, Howard RJ, Dixit VM et al. Thrombospondin binds falciparum malaria parasitized erythrocytes and may mediate cytoadherence. *Nature* [Internet]. 1985;318:64–6. Available from: <https://doi.org/10.1038/318064a0>
- Helms J, Kremer S, Merdji H, Clere-Jehl R, Schenck M, Kummerlen C et al. Neurologic Features in Severe SARS-CoV-2 Infection. *N Engl J Med* [Internet]. 2020;382:2268–70. Available from: <https://doi.org/10.1056/NEJMc2008597>
- Engelmann B, Massberg S. Thrombosis as an intravascular effector of innate immunity. *Nat Rev Immunol* [Internet]. 2012;13:34–45. Available from: <http://www.nature.com/doi/https://doi.org/10.1038/nri3345>
- Moxon CA, Wassmer SC, Milner DAJ, Chisala NV, Taylor TE, Seydel KB, et al. Loss of endothelial protein C receptors links coagulation and inflammation to parasite sequestration in cerebral malaria in African children. *Blood*. 2013;122:842–51.
- Moxon CA, Chisala NV, Mzikamanda R, MacCormick I, Harding S, Downey C et al. Laboratory evidence of disseminated intravascular coagulation is associated with a fatal outcome in children with cerebral malaria despite an absence of clinically evident thrombosis or bleeding. *J Thromb Haemost* [Internet]. 2015;13:1653–64. Available from: <https://doi.org/10.1111/jth.13060>
- Hemmer CJ, Kern P, Holst FGE, Radtke KP, Egbring R, Bierhaus A et al. Activation of the host response in human plasmodium falciparum malaria: Relation of parasitemia to tumor necrosis factor/cachectin, thrombin-antithrombin III, and protein C levels. *Am J Med* [Internet]. 1991;91:37–44. Available from: <https://www.sciencedirect.com/science/article/pii/0002934391900715>
- Vogtseder A, Ospelt C, Reindl M, Schober M, Schmutzhard E. Time course of coagulation parameters, cytokines and adhesion molecules in *Plasmodium falciparum* malaria. *Trop Med Int Heal* [Internet]. 2004;9:767–73. Available from: <https://doi.org/10.1111/j.1365-3156.2004.01265.x>
- Soldatelli MD, Amaral LF do, Veiga VC, Rojas SSO, Omar S, Marussi VHR. Neurovascular and perfusion imaging findings in coronavirus disease 2019: Case report and literature review. *Neuroradiol J* [Internet]. 2020;33:368–73. Available from: <https://doi.org/10.1177/1971400920941652>
- Siegel JS, Snyder AZ, Ramsey L, Shulman GL, Corbetta M. The effects of hemodynamic lag on functional connectivity and behavior after stroke. *J Cereb Blood Flow Metab* [Internet]. 2015;36:2162–76. Available from: <https://doi.org/10.1177/0271678X15614846>
- Semmler A, Hermann S, Mormann F, Weberpals M, Paxian SA, Okulla T, et al. Sepsis causes neuroinflammation and concomitant decrease of cerebral metabolism. *J Neuroinflammation*. 2008;5:1–10.
- Pappas G, Roussos N, Falagas ME. Toxoplasmosis snapshots: Global status of *Toxoplasma gondii* seroprevalence and implications for pregnancy and congenital toxoplasmosis. *Int J Parasitol* [Internet]. 2009;39:1385–94. Available from: <https://doi.org/10.1016/j.ijpara.2009.04.003>
- Konradt C, Ueno N, Christian DA, Delong JH, Pritchard GH, Herz J et al. Endothelial cells are a replicative niche for entry of *Toxoplasma gondii* to the central nervous system. *Nat Microbiol* [Internet]. 2016;1:16001. Available from: <https://doi.org/10.1038/nmicrobiol.2016.1>
- Marcos AC, Siqueira M, Alvarez-Rosa L, Cascabulho CM, Waghbi MC, Barbosa HS et al. *Toxoplasma gondii* infection impairs radial glia differentiation and its potential to modulate brain microvascular endothelial cell function in the cerebral cortex. *Microvasc Res* [Internet]. 2020;131:104024. Available from: <https://doi.org/10.1016/j.mvr.2020.104024>
- Estato V, Stipursky J, Gomes F, Mergener TC, Frazão-Teixeira E, Allodi S, et al. The neurotropic parasite *Toxoplasma Gondii* induces sustained neuroinflammation with microvascular dysfunction in infected mice. *Am J Pathol*. 2018;188:2674–87.
- Kovacs MA, Babcock IW, Royo Marco A, Sibley LA, Kelly AG, Harris TH. Vascular endothelial growth factor-C treatment enhances cerebrospinal fluid outflow during *Toxoplasma Gondii* Brain infection but does not improve cerebral edema. *Am J Pathol*. 2024;194:225–37.
- Figueiredo CA, Steffen J, Morton L, Arumugam S, Liesenfeld O, Deli MA et al. Immune response and pathogen invasion at the choroid plexus in the onset of cerebral toxoplasmosis. *J Neuroinflammation* [Internet]. 2022;19:17. Available from: <https://doi.org/10.1186/s12974-021-02370-1>
- Dubey JP, Speer CA, Shen SK, Kwok OC, Blixt JA. Oocyst-induced murine toxoplasmosis: life cycle, pathogenicity, and stage conversion in mice fed *Toxoplasma Gondii* oocysts. *J Parasitol*. 1997;83:870–82.
- Dubey JP. Advances in the life cycle of *Toxoplasma gondii*. *Int J Parasitol*. 1998;28:1019–24.
- Knowland D, Arac A, Sekiguchi KJ, Hsu M, Lutz SE, Perrino J et al. Stepwise Recruitment of Transcellular and Paracellular Pathways Underlies Blood-Brain Barrier Breakdown in Stroke. *Neuron* [Internet]. 2014;82:603–17. Available from: <https://www.sciencedirect.com/science/article/pii/S0896627314001974>
- Gov L, Karimzadeh A, Ueno N, Lodoen MB. Human innate immunity to *Toxoplasma gondii* is mediated by host caspase-1 and ASC and parasite GRA15. *MBio*. 2013;4:e00255–13.
- Schneider CA, Figueroa Velez DX, Azevedo R, Hoover EM, Tran CJ, Lo C et al. Imaging the dynamic recruitment of monocytes to the blood-brain barrier and specific brain regions during *Toxoplasma gondii* infection. *Proc Natl Acad Sci U S A* [Internet]. 2019;116:24796–807. Available from: <http://www.pnas.org/content/116/49/24796.abstract>
- Burg JL, Grover CM, Pouletty P, Boothroyd JC. Direct and sensitive detection of a pathogenic protozoan, *Toxoplasma gondii*, by polymerase chain reaction. *J Clin Microbiol* [Internet]. 1989;27:1787–92. Available from: <https://pubmed.ncbi.nlm.nih.gov/2768467>
- Morgado P, Ong Y-C, Boothroyd JC, Lodoen MB. *Toxoplasma gondii* induces B7-2 expression through activation of JNK signal transduction. *Infect Immun* [Internet]. 2011;09/12. 2011;79:4401–12. Available from: <https://pubmed.ncbi.nlm.nih.gov/21911468>
- Livak KJ, Schmittgen TD. Analysis of relative gene expression data using real-time quantitative PCR and the 2(-Delta Delta C(T)) method. *Methods*. 2001;25:402–8.

34. Zhu X, Huang L, Zheng Y, Song Y, Xu Q, Wang J et al. Ultrafast optical clearing method for three-dimensional imaging with cellular resolution. *Proc Natl Acad Sci U S A* [Internet]. 2019;116:11480–9. Available from: <http://www.pnas.org/content/116/23/11480.abstract>
35. Schindelin J, Arganda-Carreras I, Frise E, Kaynig V, Longair M, Pietzsch T et al. Fiji: an open-source platform for biological-image analysis. *Nat Methods* [Internet]. 2012;9:676–82. Available from: <https://doi.org/10.1038/nmeth.2019>
36. Schneider CA, Velez DXF, Orchanian SB, Shallberg LA, Agalliu D, Hunter CA et al. *Toxoplasma gondii* Dissemination in the Brain Is Facilitated by Infiltrating Peripheral Immune Cells. *MBio* [Internet]. 2022;13:e02838–22. Available from: <https://doi.org/10.1128/mbio.02838-22>
37. Ohashi T, Sugaya Y, Sakamoto N, Sato M. Hydrostatic pressure influences morphology and expression of VE-cadherin of vascular endothelial cells. *J Biomech* [Internet]. 2007;40:2399–405. Available from: <https://www.sciencedirect.com/science/article/pii/S0021929006004817>
38. Hoover EM, Crouzet C, Bordas JM, Figueroa Velez DX, Gandhi SP, Choi B et al. Transcranial chronic optical access to longitudinally measure cerebral blood flow. *J Neurosci Methods* [Internet]. 2021;350:109044. Available from: <http://www.sciencedirect.com/science/article/pii/S0165027020304672>
39. Ramirez-San-Juan JC, Ramos-Garcia R, Guizar-Iturbide I, Martinez-Nicono G, Choi B. Impact of velocity distribution assumption on simplified laser speckle imaging equation. *Opt Express* [Internet]. 2008;16:3197–203. Available from: <http://www.opticsexpress.org/abstract.cfm?URL=oe-16-5-3197>
40. Cortes-Canteli M, Mattei L, Richards AT, Norris EH, Strickland S. Fibrin deposited in the Alzheimer's disease brain promotes neuronal degeneration. *Neurobiol Aging*. 2015;36:608–17.
41. Scharf-Kersten T, Nakajima H, Yap G, Sher A, Leonard WJ. Infection of mice lacking the common cytokine receptor gamma-chain (gamma(c)) reveals an unexpected role for CD4+ T lymphocytes in early IFN-gamma-dependent resistance to *Toxoplasma gondii*. *J Immunol*. 1998;160:2565–9.
42. Yap GS, Sher A. Cell-mediated immunity to *Toxoplasma gondii*: initiation, regulation and effector function. *Immunobiology*. 1999;201:240–7.
43. Yarovinsky F. Innate immunity to *Toxoplasma gondii* infection. *Nat Rev Immunol* [Internet]. 2014;14:109–21. Available from: <http://www.nature.com/doi/10.1038/nri3598>
44. Sturge CR, Yarovinsky F. Complex immune cell interplay in the gamma interferon response during *Toxoplasma gondii* infection. *Infect Immun*. 2014;82:3090–7.
45. Deckert-Schlüter M, Bluethmann H, Kaefel N, Rang A, Schlüter D. Interferon-gamma receptor-mediated but not tumor necrosis factor receptor type 1- or type 2-mediated signaling is crucial for the activation of cerebral blood vessel endothelial cells and microglia in murine *Toxoplasma* encephalitis. *Am J Pathol* [Internet]. 1999;154:1549–61. Available from: <https://pubmed.ncbi.nlm.nih.gov/10329607>
46. Sa Q, Ochiala E, Sengoku T, Wilson ME, Brogli M, Crutcher S, et al. VCAM-1/alpha4 beta1 integrin interaction is crucial for prompt recruitment of immune T cells into the brain during the early stage of reactivation of chronic infection with *Toxoplasma gondii* to prevent toxoplasmic encephalitis. *Infect Immun*. 2014;82:2826–39.
47. Dincel GC, Atmaca HT. Increased expressions of ADAMTS-13 and apoptosis contribute to neuropathology during *Toxoplasma gondii* encephalitis in mice. *Neuropathology*. 2016;36:211–26.
48. Wang X, Michie SA, Xu B, Suzuki Y. Importance of IFN-gamma-mediated expression of endothelial VCAM-1 on recruitment of CD8+ T cells into the brain during chronic infection with *Toxoplasma gondii*. *J Interferon Cytokine Res*. 2007;27:329–38.
49. Olivera GC, Ross EC, Peuckert C, Barragan A. Blood-brain barrier-restricted translocation of *Toxoplasma gondii* from cortical capillaries. *Elife*. 2021;10.
50. Suzuki Y, Orellana MA, Schreiber RD, Remington JS. Interferon-gamma: the major mediator of resistance against *Toxoplasma gondii*. *Science*. 1988;240:516–8.
51. Gazzinelli R, Xu Y, Hieny S, Cheever A, Sher A. Simultaneous depletion of CD4+ and CD8+ T lymphocytes is required to reactivate chronic infection with *Toxoplasma gondii*. *J Immunol* [Internet]. 1992;149:175 LP-180. Available from: <http://www.jimmunol.org/content/149/1/175.abstract>
52. Hirsh J, Warkentin TE, Shaughnessy SG, Anand SS, Halperin JL, Raschke R et al. Heparin and Low-Molecular-Weight Heparin Mechanisms of Action, Pharmacokinetics, Dosing, Monitoring, Efficacy, and Safety. *Chest* [Internet]. 2001;119:64S–94S. Available from: <https://www.sciencedirect.com/science/article/pii/S0012369215607814>
53. Johnson LL, Berggren KN, Szaba FM, Chen W, Smiley ST. Fibrin-mediated Protection Against Infection-stimulated Immunopathology. *J Exp Med* [Internet]. 2003;197:801 LP-806. Available from: <http://jem.rupress.org/content/197/6/801.abstract>
54. Mullarky IK, Szaba FM, Winchel CG, Parent MA, Kummer LW, Mackman N et al. In situ assays demonstrate that interferon-gamma suppresses infection-stimulated hepatic fibrin deposition by promoting fibrinolysis. *J Thromb Haemost* [Internet]. 2006;4:1580–7. Available from: <https://doi.org/10.1111/j.1538-7836.2006.02010.x>
55. Mackman N. Tissue-specific hemostasis in mice. *Arterioscler Thromb Vasc Biol*. 2005; pp. 2273–81.
56. Rosenberg RD, Aird WC. Vascular-Bed-Specific Hemostasis and Hypercoagulable States. *N Engl J Med* [Internet]. 1999;340:1555–64. Available from: <http://www.nejm.org/doi/https://doi.org/10.1056/NEJM199905203402007>
57. Horn T, Henriksen JH, Christensen P. The sinusoidal lining cells in normal human liver. A scanning electron microscopic investigation. *Liver*. 1986;6:98–110.
58. Dejana E. Endothelial cell-cell junctions: happy together. *Nat Rev Mol Cell Biol*. 2004;5:261–70.
59. Middleton EA, He X-Y, Denorme F, Campbell RA, Ng D, Salvatore SP, et al. Neutrophil extracellular traps contribute to immunothrombosis in COVID-19 acute respiratory distress syndrome. *Blood*. 2020;136:1169–79.
60. Aikawa M, Iseki M, Barnwell JW, Taylor D, Oo MM, Howard RJ. The pathology of human cerebral malaria. *Am J Trop Med Hyg* [Internet]. 1990;43:30–7. Available from: https://www.ajtmh.org/view/journals/tpmd/43/2_Part_2/article-p30.xml
61. Crabb BS, Cooke BM, Reeder JC, Waller RF, Caruana SR, Davern KM et al. Targeted Gene Disruption Shows That Knobs Enable Malaria-Infected Red Cells to Cytoadhere under Physiological Shear Stress. *Cell* [Internet]. 1997;89:287–96. Available from: <https://www.sciencedirect.com/science/article/pii/S009286740080207X>
62. Salwen SA, Szarowski DH, Turner JN, Bizios R. Three-dimensional changes of the cytoskeleton of vascular endothelial cells exposed to sustained hydrostatic pressure. *Med Biol Eng Comput* [Internet]. 1998;36:520–7. Available from: <https://doi.org/10.1007/BF02523225>
63. Acevedo AD, Bowser SS, Gerritsen ME, Bizios R. Morphological and proliferative responses of endothelial cells to hydrostatic pressure: Role of fibroblast growth factor. *J Cell Physiol* [Internet]. 1993;157:603–14. Available from: <https://doi.org/10.1002/jcp.1041570321>
64. Li Y, Choi WJ, Wei W, Song S, Zhang Q, Liu J et al. Aging-associated changes in cerebral vasculature and blood flow as determined by quantitative optical coherence tomography angiography. *Neurobiol Aging* [Internet]. 2018;70:148–59. Available from: <http://www.sciencedirect.com/science/article/pii/S0197458018302215>
65. Darbousset R, Thomas GM, Mezouar S, Frère C, Bonier R, Mackman N, et al. Tissue factor-positive neutrophils bind to injured endothelial wall and initiate thrombus formation. *Blood*. 2012;120:2133–43.
66. Pawlinski R, Wang J-G, Owens AP 3rd, Williams J, Antoniak S, Tencati M, et al. Hematopoietic and nonhematopoietic cell tissue factor activates the coagulation cascade in endotoxemic mice. *Blood*. 2010;116:806–14.
67. Johnson LL, Berggren KN, Szaba FM, Chen W, Smiley ST. Fibrin-mediated protection against infection-stimulated immunopathology. *J Exp Med* [Internet]. 2003;197:801–6. Available from: <http://www.pubmedcentral.nih.gov/articlerender.fcgi?artid=2193855&tool=pmcentrez&rendertype=abstract>

Publisher's note

Springer Nature remains neutral with regard to jurisdictional claims in published maps and institutional affiliations.